

Colour Appearance Rating of Familiar Real Objects

Kevin Smet,^{1*} Wouter R. Ryckaert,¹ Michael R. Pointer,²
Geert Deconinck,³ Peter Hanselaer¹

¹Light and Lighting Laboratory, Department of Physics, Catholic University College Gent, Belgium

²Department of Colour Science, University of Leeds, Leeds, United Kingdom

³ESAT/ELECTA, K.U. Leuven, Leuven, Belgium

Received 18 January 2010; revised 16 February 2010; accepted 19 February 2010

Abstract: The determination of the long-term memory colours of objects has been the subject of investigation for many years. Colour acceptance boundaries have been determined from the visual assessments of objects under variable illumination or by presenting manipulated images of objects on a calibrated computer display. However, a systematic and quantitative rating of the colour of real objects with respect to memory colour is not available at this moment. In this article, nine familiar real objects with colours distributed around the hue circle were positioned in a specially designed LED illumination box. For each object, approximately hundred real illumination spectra were synthesized in a random order keeping the luminance of the object approximately constant. Observers were asked to rate, on a five-point scale, the similarity of the perceived object colour to their idea of what the object looked like in reality. By avoiding specular reflections, the observer was unable to identify any clues as to the colour of the illumination. For each object, similarity ratings showed a good intraobserver and interobserver agreement. The ratings of all the observers were pooled and successfully modeled in IPT colour space by a bivariate Gaussian distribution. It was found that the chromaticity corresponding to the highest rating tended to be shifted toward higher chroma in comparison with the chromaticity calculated under D65 illumination. The bivariate distributions could be very useful in applications where the quantitative evaluation of the colour appearance of an object stimulus is required, such as in the evaluation of the colour rendering capabilities of a light source. © 2010 Wiley Periodicals, Inc. *Col Res Appl*,

36, 192–200, 2011; Published online 21 June 2010 in Wiley Online Library (wileyonlinelibrary.com). DOI 10.1002/col.20620

Key words: color appearance; memory colors; familiar objects; real objects; psychophysical experiments; color rendering; led lighting

INTRODUCTION

In 1920, Hering stated that the world is viewed through the spectacles of memory.¹ Indeed, the perception and preference of the colour of familiar objects is judged with respect to the memory colour associated with that object. For many decades, memory colours and corresponding preferences have been studied extensively.^{2–13} The concept of memory colour is important in many areas of colour research, such as colour reproduction^{4,6,10,11,14} and colour rendering.^{15–17} In both applications, memory colours can be used as an internal reference to assess colour appearance. Judd's flattery index¹⁷ and Thornton's colour preference index¹⁶ were based on the memory data obtained by Sanders⁵ and Newhall *et al.*² In 1965, the International Commission on Illumination (CIE) recommended a colour rendering index based on the Test Colour Method^{18–20} with the use of a reference illuminant, thereby ignoring the use of memory colours as a potential internal reference. Recently, increasing evidence suggests that the CIE Test Colour Method fails to predict the actual visual rendering abilities of typical narrow-band light sources such as light emitting diodes (LEDs)^{21–25} and tri-band fluorescent lamps.^{26,27} Colour rendering has again become an important research topic, offering an opportunity to reconsider a memory colour approach.

Until now, research on the memory colours of real objects has been limited to the determination of the chromaticity shift with respect to object colours under a natural illumination.^{2–4,6,7,13,28} Bodrogi and Tarczali^{10,11}

*Correspondence to: Kevin Smet (e-mail: kevin.smet@kahosl.be).

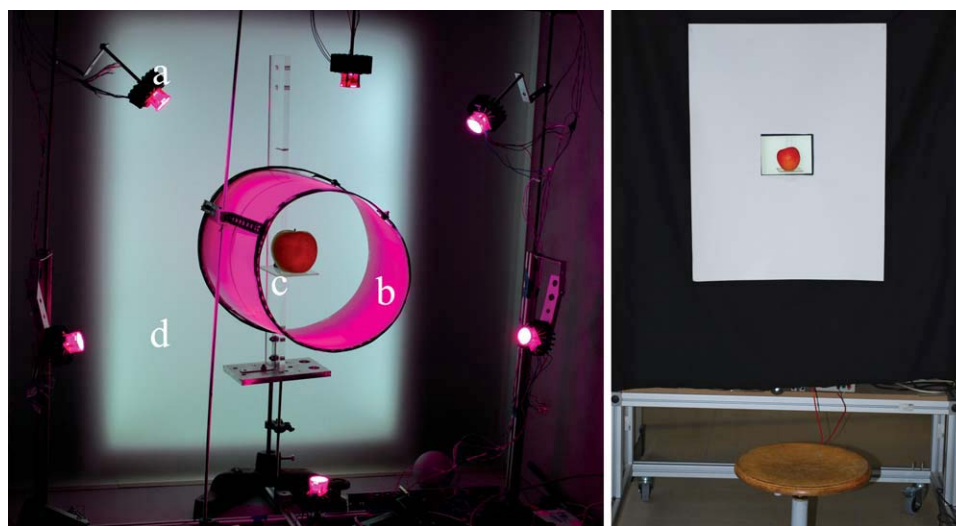


FIG. 1. Left: Interior of the illumination box: (a) RGB LEDs; (b) diffusing tunnel; (c) transparent support for the object; (d) self luminous back panel. Right: An object inside the illumination box as seen by the observer.

and Sanders⁵ established, respectively, constant domains and tolerances for the memory colours of each of the objects they considered. These domains or tolerances can indicate acceptability limits (pass/fail), but do not provide the necessary detail to enable a quantitative assessment of the colour appearance of the object. Yendrikhovskij *et al.*⁸ did provide a complete description of how observers would rate the appearance of an object by modeling the colour appearance ratings of the object, but unfortunately only a ripe banana was modeled. Furthermore, the ratings were obtained by displaying familiar objects on a computer display^{8–11} or by using an abstract cue, such as the object name, without image context.^{3,4,7} However, it has been demonstrated that the naturalness of object representation, providing information on surface texture, shading, motion parallax, and binocular disparity,²⁹ has an influence on similarity ratings⁸ and on colour constancy.^{30,31} Self-luminous displays look different from what colorimetry predicts,³² and in a recent article Oicherman *et al.*³³ stated that colorimetric matches between computer displays and surface colours do not necessarily result in perceptual matches. Finally, experiments performed by Fairchild pointed to a difference in chromatic adaptation between hard-copy and soft-copy displays.³⁴

This article presents the results of colour appearance assessments of a set of familiar real objects with respect to observer memory colour. For each object, approximately 100 illumination conditions were selected in a random order. Observers were asked to rate the similarity of the presented object colour with their idea (memory) of what the object looks like in reality. These experiments provide quantitative data of colour appearance ratings referenced to memory colours.

MATERIALS AND METHODS

Illumination Box

To achieve reliable colour appearance ratings, observers should not be able to identify the colour of the illumina-

tion, but be given the impression that the objects themselves change colour. With this in mind, a special illumination box with some particular features was constructed such that real objects could be illuminated with combinations of Red, Green, Blue, and Amber (RGBA) LEDs.

The interior and exterior of the illumination box are shown in Fig. 1. The dimensions are 106 cm (width) \times 112 cm (height) \times 74 cm (depth). The walls were painted neutral Munsell N4 gray. The illumination was provided by a set of six RGBA LED packages connected to a pulse-width modulated (PWM) current driven power supply controlled by a LabVIEW[®] program. The LED packages were mounted on a heat sink to stabilize their temperature.

To illuminate the objects uniformly and to mask the specular reflection spot which would reveal the illumination colour, the RGBA LED packages were mounted around a diffusing tunnel. The object was placed inside this diffusing tunnel on a support, which was chosen to be transparent to ensure that no surface reflections from the LED illumination are visible.

At the back of the illumination box, a self-luminous white panel with a correlated colour temperature of approximately 5600 K, 1964 chromaticity coordinates x_{10} , $y_{10} = 0.3289$, 0.3514 and a luminance of 590 cd m^{-2} was mounted to ensure a constant adaptation state irrespective of the colour of the LED illumination.³⁴

Finally, the illumination box was closed by a front panel that left only a central 10° viewing aperture. The outer side of the front panel was illuminated by an external fluorescent lamp. In this way, the chromaticity of the front panel was approximately the same as the chromaticity of the back panel ($x_{10} = 0.3304$, $y_{10} = 0.3535$). The eye adaptation state was therefore assumed to be maintained.

Spectral Measurements

The spectral radiance of the objects was determined using a Bentham telespectroradiometric measuring head

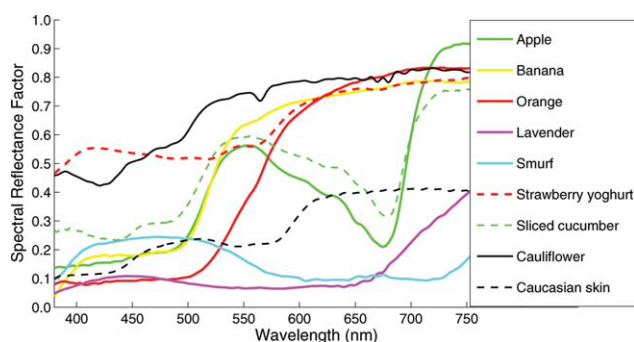


FIG. 2. Spectral reflectance factors of the nine familiar objects.

coupled to an Oriel Instruments 74055 MS260i spectrograph and an iDUS DV420A-BU2 CCD detector, similar to the hardware configuration used by Hanselaer *et al.*³⁵ A spectral bandwidth of 2.5 nm allowed for accurate determination of CIE 10 degree observer trichromatic values and associated coordinates.³⁶ The measuring geometry was similar to the viewing geometry used in the experiments.

Objects

Test objects having hues distributed around the hue circle were selected. Green, yellow, and orange familiar objects were easy to find: a green apple and a sliced cucumber, a ripe banana and an orange. Red, purple, and blue objects were, however, more problematic. Red objects were not selected because the variation in object chromaticity obtained with any of the LED illumination settings was very limited due to the highly saturated colour of most natural red objects. Strawberry yoghurt was therefore chosen to sample the red part of the hue circle. Preliminary tests with blue flowers (asters) revealed that different observers have different versions of the same object in mind, resulting in an unacceptable interobserver consistency. Observers also reported that it was difficult to keep a fixed reference memory colour in their mind. A smurf[®] figurine was therefore selected as a blue test object. The value of the interobserver consistency confirmed that indeed many observers did seem to have a reasonably good memory of the colour of a smurf[®]. After preliminary tests with several purple objects (grapes, flowers,...), dried lavender was selected. Finally, two special objects were added to the set. A cauliflower was added to cover neutral colours, and a life-like silicon hand was added to rate Caucasian skin, because of the critical nature of its colour in many practical applications.

The mean spectral reflectance factors of the nine test objects were calculated from the measured spectral radiance of the objects illuminated with a halogen light source. A CERAM ceramic white tile was used as reference standard. These results are shown in Fig. 2.

No food degradation was observed as the experiments with one object were efficiently organized to take place on the same day.

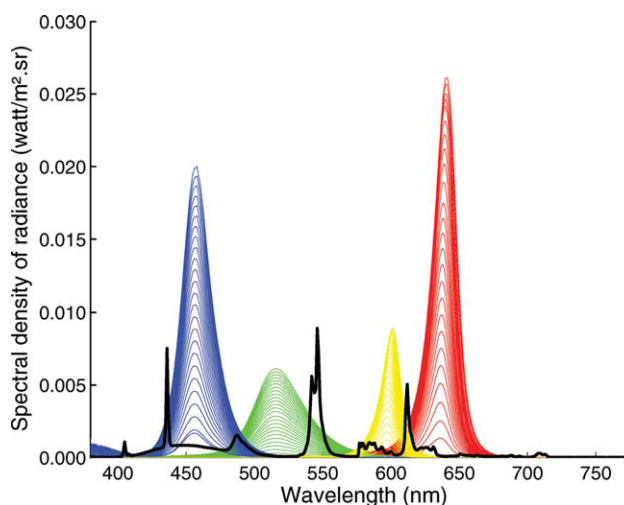


FIG. 3. Spectral radiance of a neutral gray-painted sphere illuminated by the back panel (black) and RGBA LEDs each powered from 0 to maximum power in steps of 10 digital units.

Illumination Box Characterization

The spectra of the monochrome LEDs and of the back panel were determined indirectly by placing a Styrofoam[®] sphere at the object location. The sphere was coated with neutral gray paint and the spectral radiance was measured using the measurement set-up described above. The results are shown in Fig. 3.

With the LEDs at maximum power, the luminance of the front side of the gray sphere reached a value of 160 cd/m². The corresponding vertical illuminance was 1150 lux. With the LEDs turned off, the luminance and the illuminance originating from the back panel decreased to 60 cd/m² and 430 lux, respectively. The contribution of

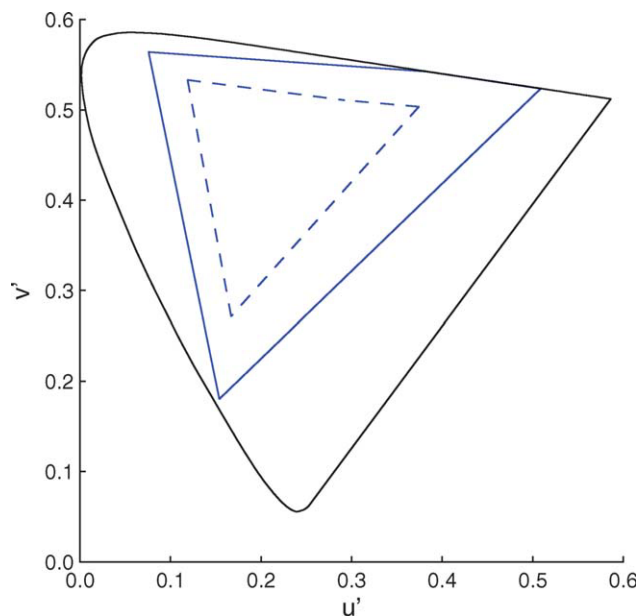


FIG. 4. RGB LED u',v' chromaticity gamut without back-panel illumination (solid blue line), gamut with back-panel illumination (broken blue line).

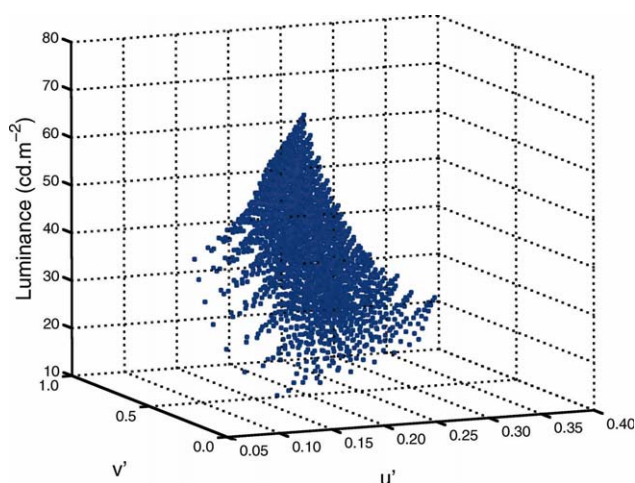


FIG. 5. Smurf® colour solid in $u'v'Y$ colour space. [Color figure can be viewed in the online issue, which is available at wileyonlinelibrary.com.]

the white back panel evidently reduces the illumination colour gamut, as illustrated in Fig. 4. The uniformity of illumination, assessed by measuring the luminance at several locations across the neutral gray sphere, was better than 90% of the maximum measured luminance.

Object Stimuli

A four-dimensional set of RGBA illumination settings was synthesized for each object. The RGBA digital-to-analog conversion (DAC) input values were sent to the PWM controller and ranged from 0 to 255, resulting in over 4 billion (256^4) possible combinations. Random selection of RGBA DAC values was not considered an option because, depending on the spectral reflectance factors of the object, the resulting object chromaticity grid could be nonuniform and the object luminance variation would be too high. A nonuniform grid could reduce the precision of the data. A large variation in object luminance might influence the visual ratings directly: a low rating of some particular object colour might be due to a low luminance and not to an unsatisfying object chromaticity.³⁷ To resolve this problem, a linear mapping of RGBA DAC values to XYZ tristimulus values was performed for each object, enabling the calculation of the colour solid of each object in any colour space. An example of a $u'v'Y$ colour solid is shown in Fig. 5. Inspection of the colour solid allows for the selection of an equal luminance plane corresponding with the largest possible chromaticity gamut. Inverse mapping was used to determine the set of RGBA DAC values resulting in an approximately uniform chromaticity grid at the selected luminance plane.

Out of this set of RGBA DAC values, 20 values were randomly selected and added to provide a check for observer consistency. This sequence of approximately 100 points was then randomized and a training set of 20 points was added to help to familiarize the observers with the procedure and the rating scale. Finally, each sequence

was applied to the LED drivers and the resulting spectral radiance of the object was measured with the measuring head positioned at the viewing position. In this way, accurate spectral radiances of the real visual stimuli presented to the observers were obtained. The repeatability of the illumination settings and of the spectral measurements was tested by comparing the u',v' colour coordinates obtained before and after a visual test experiment. The colour differences were smaller than 0.003. Luminance data were calculated and are summarized in Table I. The average standard deviation of each sequence was $\pm 4\%$ with a maximum value of $\pm 8\%$.

Tristimulus values were calculated using the CIE 1964 standard observer because the objects had an angular subtense larger than 4° . The tristimulus values were transformed to corresponding colours under a D65 illuminant using the CAT02 chromatic adaptation transform. Afterward, chromaticities were transformed to the IPT colour space developed by Ebner and Fairchild.³⁸ CIECAM02 colour appearance space could not be used because it is unable to model appearance in the presence of a self-luminous background, which would require the Y_b parameter to be larger than 100. IPT space, however, is an opponent colour space with achromatic (I), red–green (P), and yellow–blue (T) channels, as well as good hue uniformity.³⁸ The IPT object grid points are shown in Fig. 6 for each of the nine objects.

Observers

A total of 32 observers (16 female and 16 male) with ages ranging from 18 to 53, participated in the visual experiments. All observers were screened for colour deficiency using the Ishihara 24-plate test. Not all observers rated each object, but each object was scaled by at least 10 observers.

Test Procedure

All observers received written instructions before starting the experiment, explaining that a familiar object (e.g., a green apple, a ripe banana, ...) would be presented several times, each time having a particular colour. They were asked to rate the colour of the object in comparison

TABLE I. Mean luminance of the test objects under a predefined sequence of LED driver settings.

Object	Mean luminance (cd/m ²)	Standard deviation luminance (cd/m ²)
Apple	95	5
Banana	99	6
Orange	83	4
Lavender	15	1
Smurf®	38	3
Strawberry yoghurt	160	2
Sliced cucumber	152	4
Cauliflower	161	3
Caucasian hand	82	3

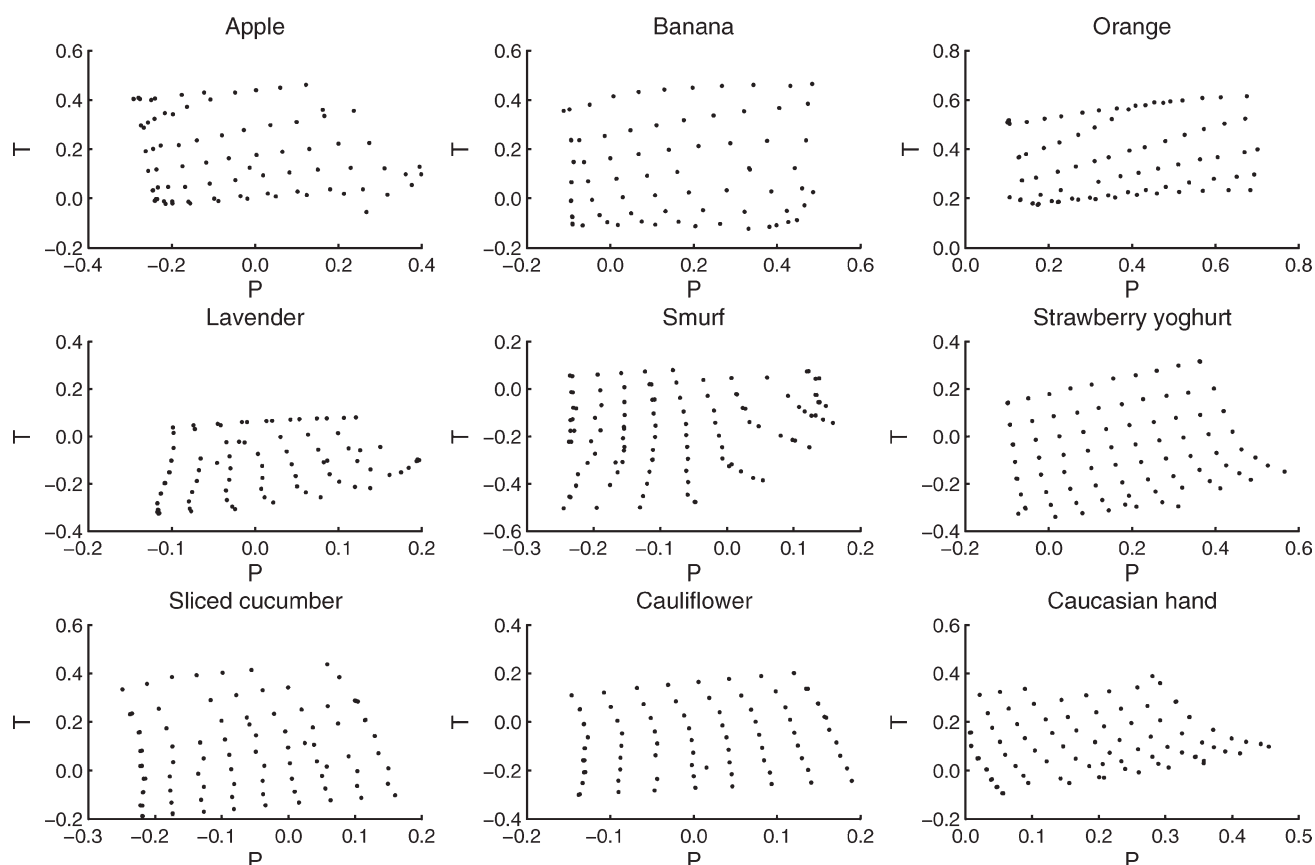


FIG. 6. IPT object chromaticities for each of the nine objects: P and T are the red–green and the yellow–blue axes of the IPT opponent colour space, respectively.

with what they thought the object should look like, on a 5 point summative response scale; 5, very good; 4, good; 3, neutral; 2, bad; and 1, very bad. This type of scale allows for the calculation of mean ratings,³⁹ enabling a direct comparison of the individual ratings of each observer with that of an average observer. It was suggested to not stare at the objects but to have a look and rate intuitively. To avoid observers being tuned by the previous object presentation, they were asked to look at the white surround of the front panel while the illumination was changed. Because of the identical chromaticity of the front panel and the back panel, the eye adaptation state was maintained. It took about 15 min for an observer to finish a sequence. Including more set points might improve the accuracy of the experiments, but it would have taken too long for the observers to rate them, leading to fatigue. None of the observers rated more than one object on any day.

RESULTS AND DISCUSSION

Intraobserver and Interobserver Variability

Intraobserver and interobserver variability were analyzed using the PF/3 performance factor. PF/3 describes the agreement between two data sets, with a value of zero implying perfect agreement. By choosing PF/3 to estimate observer accuracy, comparison with the results of colour discrimination studies^{40–43} was possible.

Interobserver PF/3 was calculated for each object with respect to the mean of all observers and ranged from 31 to 45 with an average of 40 (Table II). These results are higher than the PF/3 values obtained in typical colour discrimination studies,^{40–43} where 30 PF/3 units are common. This finding is not surprising considering that the observers were rating colour appearance against their medium or long-term memory colour, which obviously could be different for each observer. It seems that the variability of the observer's internal memory colour contributes to an additional observer variability of only 10 PF/3 points.

The intraobserver PF/3 repeatability was calculated from the results of observers repeating the experiment

TABLE II. Interobserver and intraobserver PF/3 measures and values for ICC(2,n) estimating the “average observer” reliability for nine familiar objects.

Object	Interobserver PF/3	Intraobserver PF/3	ICC(2,n)
Apple	45	19	0.91
Banana	31	19	0.97
Orange	37	24	0.92
Lavender	45	30	0.86
Smurf [®]	41	24	0.91
Strawberry Yoghurt	41	25	0.90
Sliced Cucumber	40	24	0.90
Cauliflower	41	22	0.94
Caucasian hand	42	21	0.94

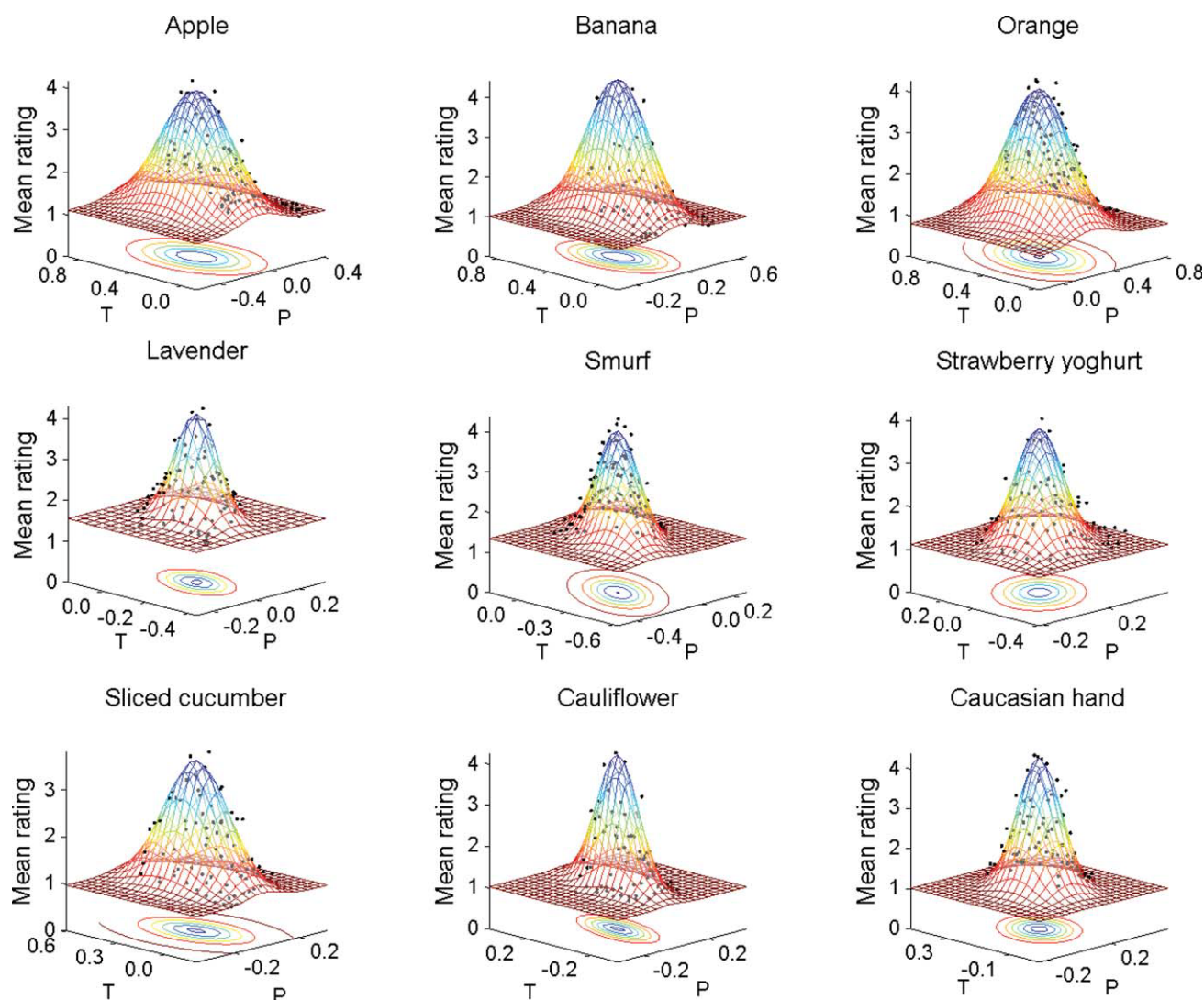


FIG. 7. Bivariate Gaussian distributions $R(P,T)$ and their d-contour ellipses obtained by fitting the pooled ratings in IPT colour space for each object. The mean rating for each illumination setting is also shown as a point to visualize the goodness-of-fit.

on a different day and with exclusion of the points introduced to check for internal rating consistency. Values ranged from 19 to 30, with an average of 23 (Table II), which is only slightly higher than intra PF/3 values obtained in colour discrimination studies.^{40–43} Internal rating consistency, calculated as the percentage of repeat grid points having the same rating, was found to be 89%, averaged over all objects and all observers.

An Intraclass Correlation Coefficient (ICC) was calculated as described by Shrout and Fleiss.⁴⁴ The ICC assesses the consistency of measurements made by multiple observers measuring the same quantity. There are six

types of ICC. ICC(2,n) was selected because it expresses the reliability of the concept of an average observer based on the ratings of a limited number of individual observers. The results are summarized in Table II. The “good” (≥ 0.75) to “excellent” (≥ 0.90) ICC(2,n) values indicate that an average observer can be postulated and that it is relevant to pool the data of all the observers.

Modeling Colour Appearance Ratings

In the past, ellipses have been used to represent the yes/no boundary for the acceptability of memory colours.^{5,10} A logical extension to ellipses, incorporating

TABLE III. Pearson correlation coefficient and RMSE between the ratings and the bivariate Gaussian function.

Object	Apple	Banana	Orange	Lavender	Smurf®	Strawberry yoghurt	Sliced cucumber	Cauliflower	Caucasian hand
ρ	0.96	0.98	0.94	0.94	0.96	0.95	0.96	0.97	0.95
RMSE	0.21	0.20	0.29	0.25	0.23	0.25	0.21	0.22	0.27

TABLE IV. Location of the memory colour of each object in IPT space.

Object	Apple	Banana	Orange	Lavender	Smurf [®]	Strawberry yoghurt	Sliced cucumber	Cauliflower	Caucasian hand
<i>P</i>	-0.0968	0.1512	0.3062	0.0150	-0.1271	0.1655	-0.0399	0.0314	0.1438
<i>T</i>	0.3802	0.3551	0.4594	-0.1403	-0.2302	-0.0132	0.2033	0.0245	0.1132

Memory colours are calculated as the centroid of the bivariate Gaussian distribution fitted to the pooled observer ratings.

quantitative ratings, is the bivariate Gaussian distribution, well known in statistics.⁴⁵ A slightly modified bivariate Gaussian distribution $R(P,T)$, described by Eq. (1), was therefore fitted to the pooled colour appearance ratings using the MATLAB `lsqcurvefit` function. Each pool of ratings (one per object) consisted of at least 1000 ratings (minimum 10 observers \times 100 illumination grid settings).

$$\begin{aligned}
 R(P,T) &= a_1 + a_2 \cdot S(P,T); \\
 S(P,T) &= \exp\left(-\frac{1}{2}(d^2(P,T))\right); \\
 d^2(P,T) &= (X - X_c)^T \cdot \sum^{-1} \cdot (X - X_c); \\
 X &= \begin{pmatrix} P \\ T \end{pmatrix}; \quad X_c = \begin{pmatrix} a_3 \\ a_4 \end{pmatrix}; \quad \sum^{-1} = \begin{bmatrix} a_5 & a_7 \\ a_7 & a_6 \end{bmatrix};
 \end{aligned} \tag{1}$$

The model requires seven parameters: a_1 and a_2 to scale the ratings and a_3 to a_7 to describe the similarity distribution $S(P,T)$. The distribution center X_c , representing the most likely location of the memory colour, is located at (a_3, a_4) , whereas the shape and orientation of

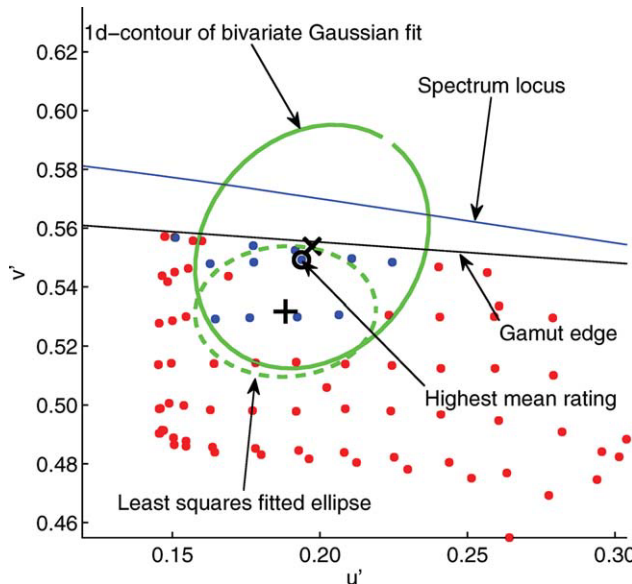


FIG. 8. Experimental results obtained for an orange. The spectrum locus for the 10° observer and the gamut edge are plotted respectively as a blue and black line. Red dots indicate grid points with a rating lower than three; blue dots have ratings higher than three. The least squares fitted ellipse is shown as the dashed green line, whereas the 1d-contour of the fitted bivariate Gaussian distribution is plotted as a solid green line. From the figure it is clear that the highest mean rating (O) is predicted more accurately by the centroid of the bivariate Gaussian distribution (X) than by the center of the least squares fitted ellipse (+).

the distribution is determined by the inverse of the covariance matrix Σ . The function $d(P,T)$ describes the elliptical d-contours of the bivariate Gaussian surface in IPT space and is often referred to as the Mahalanobis distance.

The results are plotted in Fig. 7 for each object. The mean ratings for each setting are also shown as dots to visualize the goodness-of-fit. The goodness-of-fit was determined by calculating the Pearson correlation coefficient ρ (confidence level $\alpha = 0.05$). The root-mean-square-error (RMSE) between the ratings predicted by the bivariate Gaussian similarity function R and the mean ratings of the pooled data was also calculated. Results for the individual objects are summarized in Table III. The average Pearson correlation was 0.96, whereas the average RMSE was 0.24. The high correlation coefficient combined with the good interobserver PF/3 and ICC(2,n) suggests that judgments of an average observer can be adequately modeled by a bivariate Gaussian function. The chromaticity of the memory colours of the selected objects are summarized in Table IV.

The adoption of a 5-point rating scale and the use of a distribution to fit the data enables a quantitative evaluation of the colour appearance of an object. This approach offers some advantages compared with a “yes or no” acceptability rating where only the “yes” ratings are modeled by an ellipse in a suitable chromaticity space.⁵ Fitting a distribution is more stable and accurate, and much less susceptible to outliers because all data points

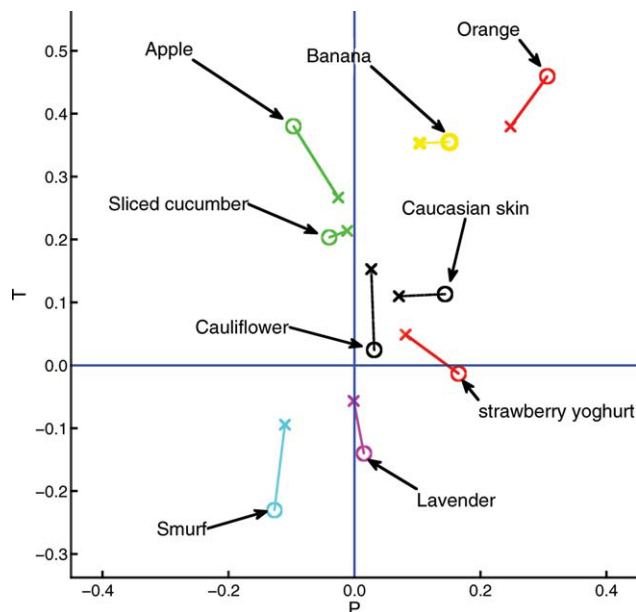


FIG. 9. Memory colours (O) and object colours rendered using CIE illuminant D65 (x).

are used. Furthermore, the need for a grid where high rated chromaticities are fully enclosed by low-rated values becomes much less critical. This becomes particularly important when the chromaticity of the centroid lies close to the edge of the gamut, as illustrated in Fig. 8. Ratings of an orange exceeding a value of 3 are indicated as blue points in the u',v' chromaticity diagram. A least squares fit of an ellipse to these points has also been drawn. The higher ratings are observed close to the edge of the gamut (black line). However, the ellipse is limited by the grid. As a consequence, a centroid lying close to the gamut edge will be very unlikely. In Fig. 8, contour ellipses of constant d calculated from the bivariate Gaussian distribution are also indicated. The 1-d contour is similar to the least squares ellipse, but the position of the distribution centroid clearly deviates from the position of the centroid of the least squares ellipse. The memory colour calculated from the distribution lies closer to the highest observed mean rating and seems to be more saturated. Similar effects were also observed for other objects.

Memory Colour and Colour Under CIE D65 Illuminant

It is of interest to compare the chromaticities of the memory colours with those of the objects using CIE illuminant D65. In Fig. 9, the object colours using D65 and the memory colours of the objects have been plotted in the PT plane of the IPT colour space.

Memory colours tend to be shifted toward higher chroma with the exception of that for the cauliflower. The memory colour associated with the smurf[®] is indeed more chromatic and bluer than it would appear under D65 illumination. Caucasian skin is also found to be remembered as more chromatic and with a slightly redder hue, in accordance with the results of Sanders.⁵ These shifts in chromaticities confirm the findings of Bartleson, who found that memory colours tend to shift toward “the most impressive chromatic attribute” of the familiar object, which is often more chromatic than the actual colour and not necessarily of the same hue.³ Several others studies have found a similar effect.^{2,4,6,8,10}

The shape and orientation of the similarity distributions suggest that, in general, observers are more tolerant toward chroma shifts than they are toward hue shifts. This justifies the use of the IPT colour space with its excellent hue uniformity.^{38,46,47}

CONCLUSIONS

This article reports on a systematic and quantitative colour appearance rating of familiar real objects. Nine objects with colours distributed around the hue circle (a green apple, a ripe banana, an orange, dried lavender, a smurf[®] figurine, strawberry yoghurt, a sliced cucumber, a cauliflower, and a Caucasian skin hand) were subsequently positioned in a specially designed LED illumination box. The observer was not able to identify the colour of the illumination by avoiding specular reflections. For each object, approximately hundred illumination spectra

were selected in a random order, keeping the luminance of the object constant within $\pm 10\%$. Thirty-two observers rated the colour appearance of the objects with respect to their idea of what the object should look like. Intraobserver and interobserver variability allowed for pooling of individual data, which were successfully modeled in IPT colour space by a bivariate Gaussian distribution. This approach enables a quantitative rating of the colour appearance of the selected objects and overcomes limitations typically associated with least squares ellipse fitting. The chromaticity of the centroid of the distribution indicates that the memory colours associated with the objects tend to be shifted toward higher chroma compared with the object colour as calculated using CIE illuminant D65. The orientation and shape of the distribution suggest that observers are more tolerant for deviations in chroma than they are for hue.

The distributions associated with these nine objects should be useful in developing a new metric for the assessment of the colour rendering capabilities of a light source. The chromaticity of the object rendered by a test source can be as input of the distribution to rate the correspondence with respect to the memory colour. Although the actual CIE recommendation for calculating a colour rendering index is based on the Test Colour Method^{19,20} and the use of a reference illuminant, an approach based on the distribution values obtained for the test objects under the test illuminant could be proposed. This approach will be investigated in a further paper.

1. Fairchild MD. Color Appearance Models, 2nd edition. Chichester: Wiley; 2005. p 158.
2. Newhall SM, Burnham RW, Clark JR. Comparison of successive with simultaneous color matching. *J Opt Soc Am* 1957;47:43–54.
3. Bartleson CJ. Memory colors of familiar objects. *J Opt Soc Am* 1960;50:73–77.
4. Bartleson CJ. Color in memory in relation to photographic reproduction. *Phot Sci Eng* 1961;5:327–331.
5. Sanders CL. Colour preferences for natural objects. *Illum Eng* 1959; 54:452–456.
6. Siple P, Springer RM. Memory and preference for the colors of objects. *Percept Psychophys* 1983;34:363–370.
7. Pérez-Carpinell J, de Fez MD, Baldoví R, Soriano JC. Familiar objects and memory color. *Color Res Appl* 1998;23:416–427.
8. Yendrikhovskij SN, Blommaert FJJ, de Ridder H. Representation of memory prototype for an object color. *Color Res Appl* 1999;24:393–410.
9. Bodrogi P, Tarczali T. Corresponding colors: The effect of color memory. *Colour Image Science CIS'2000 Conference*, Derby, UK, 2000.
10. Bodrogi P, Tarczali T. Colour memory for various sky, skin, and plant colors: Effect of the image context. *Color Res Appl* 2001;26: 278–289.
11. Bodrogi P, Tarczali T. Investigation of color memory. In: MacDonal LW, Luo MR, editors. *Colour Image Science: Exploiting Digital Media*. Chichester: Wiley; 2002. p 23–48.
12. Hurlbert AC, Ling Y. If it's a banana, it must be yellow: The role of memory colors in color constancy. *J Vision* 2005;5:787–787.
13. Olkkonen M, Hansen T, Gegenfurtner KR. Color appearance of familiar objects: Effects of object shape, texture, and illumination changes 2008;8:1–16.
14. Yendrikhovskij SN, Blommaert FJJ, de Ridder H. Color reproduction and the naturalness constraint. *Color Res Appl* 1999;24:52–67.

15. Sanders CL. Assessment of color rendition under an illuminant using color tolerances for natural objects. *Illum Eng* 1959;54:640–646.
16. Thornton WA. A validation of the color preference index. *Illum Eng* 1972;62:191–194.
17. Judd DB. A flattery index for artificial illuminants. *Illum Eng* 1967;62:593–598.
18. CIE Publ. 13 (E–1.3.2). Method of Measuring and Specifying Colour Rendering Properties of Light Sources. Paris: CIE Central Bureau; 1965.
19. CIE Publ. 13.2. Method of Measuring and Specifying Colour Rendering Properties of Light Sources. Paris: CIE Central Bureau; 1974.
20. CIE Publ. 13.3. Method of Measuring and Specifying Colour Rendering Properties of Light Sources. Vienna: CIE Central Bureau; 1995.
21. Bodrogi P, Csuti P, Hotváth P, Schanda J. Why does the CIE color rendering index fail for white RGB LED light sources? CIE Expert Symposium on LED Light Sources: Physical Measurement and Visual and Photobiological Assessment, Tokyo, Japan, 2004.
22. Davis W, Ohno Y. Toward an improved color rendering metric in Fifth International Conference on Solid State Lighting. In: Ferguson IT, Carrano JC, Taguchi T, Ashdown IE, editors. *Proc of SPIE 5941*. Bellingham, WA: SPIE; 2005. p G1–G8.
23. Szabó F, Schanda J, Bodrogi P, Radkov E. A comparative study of new solid state light sources. CIE Session, 2007.
24. Narendran N, Deng L. Color rendering properties of LED light sources. Solid state lighting II. Proceedings of SPIE, 2002.
25. Tarczali T, Bodrogi P, Schanda J. Colour rendering properties of LED sources. CIE 2nd LED Measurement Symposium, Gaithersburg, 2001.
26. Thornton WA. Luminosity and color-rendering capability of white light. *J Opt Soc Am* 1971;61:1155–1163.
27. Valberg A, Seim T, Sällström P. Colour rendering and the three-band fluorescent lamp. Meeting of the CIE 1979, Kyoto, Japan, 1979.
28. Pérez-Carpinell J, Camps VJ, de Fez MD, Castro J. Color memory matching in normal and red-green anomalous trichromat subjects. *Color Res Appl* 2001;26:158–170.
29. Ling Y, Hurlbert A. Color and size interactions in a real 3D object similarity task. *J Vision* 2004;4:721–734.
30. Berns RS, Gorzynski ME. Simulating surface colors on CRT displays: The importance of cognitive clues. *AIC Colour and Light*, Volume 91, 1991. p 21–24.
31. Brainard DH. Color constancy in the nearly natural image, Part 2: Achromatic loci. *J Opt Soc Am A* 1998;15:307–325.
32. Hunt RWG. *The Reproduction of Colour*. Chichester: Wiley; 2004.
33. Oicherman B, Luo MR, Rigg B, Robertson AR. Adaptation and color matching of display and surface colors. *Color Res Appl* 2009;34:182–193.
34. Fairchild MD. Chromatic adaptation to image displays. *TAGA* 1992;2:803–824.
35. Hanselaer P, Keppens A, Forment S, Ryckaert WR, Deconinck G. A new integrating sphere design for spectral radiant flux determination of light-emitting diodes. *Meas Sci Technol* 2009;20.
36. Ohno Y. Spectral color measurement. In: Schanda J, editor. *Colorimetry: Understanding the CIE System*. Vienna, Austria: CIE Central Bureau; 2007. p 5.1–5.30.
37. Smet K, Ryckaert WR, Forment S, Deconinck G, Hanselaer P. Colour rendering: An object based approach. CIE Light and Lighting Conference with Special Emphasis on LEDs and Solid State Lighting, Volume 1, Budapest, Hungary, 2009.
38. Ebner F, Fairchild MD. Development and testing of a color space (IPT) with improved hue uniformity. *IS&T 6th Color Imaging Conference*. Springfield, VA: IS&T; 1998. p 8–13.
39. Meyers LS, Gamst G, Guarino AJ. *Scales of Measurement. Applied Multivariate Research: Design and Interpretation*. Thousand Oaks, CA: Sage; 2006. p 20–23.
40. Guan S-S, Luo MR. A color-difference formula for assessing large color differences. *Color Res Appl* 1999;24:344–355.
41. Guan S-S, Luo MR. Investigation of parametric effects using large color differences. *Color Res Appl* 1999;24:356–368.
42. Guan S-S, Luo MR. Investigation of parametric effects using small color differences. *Color Res Appl* 1999;24:331–343.
43. Xu H, Yaguchi H, Shiori S. Estimation of color-difference formulae at color discrimination threshold using CRT-generated stimuli. *Opt Rev* 2001;8:142–147.
44. Shrout PE, Fleiss JL. Intraclass correlations: Uses in assessing rater reliability. *Psychol Bull* 1979;2:420–428.
45. NIST/SEMATECH. e-Handbook of statistical methods, The Multivariate Normal Distribution. Available at: <http://www.itl.nist.gov/div898/handbook/pmc/section5/pmc542.htm>. Accessed 2010, Jan 11th.
46. Fairchild MD, Garrett JM. Image appearance modeling. *SPIE/IS&T Electronic Imaging Conference*, Volume 5007, Santa Clara, 2003. p 149–160.
47. Jin H, Zhao X, Liu H. Testing of the uniformity of color appearance space. *World Congress on Computer Science and Information Engineering*, CSIE. Volume 6, 2009. p 307–311.

NEWS

Munsell Color Science Laboratory: Industrial Short Courses 2011

Essentials of Color Science, June 14–15, 2011

Advanced Topics in Color and Imaging, June 16, 2011

Instrumental-Based Color Matching, June 16, 2011

This year's courses, held at Rochester Institute of Technology (RIT), are sure to please! "Essentials of Color Science" is a 2-day short course composed of eight lectures, all designed to teach you the theory and application of modern color science. The faculty and staff of Munsell Color Science Laboratory (MCSL) are your teachers, all experts in these many facets of color.

For the first time, we have added two 1-day courses, offered simultaneously, so you will have to choose! "Advanced Topics in Color and Imaging" consists of four lectures in topical areas, where our faculty have had significant impact in imaging technology. "Instrumental-Based Color Matching" is a hands-on course with both lectures and laboratories, where you will gain a deeper understanding of what goes on "under the hood" of commercial matching systems.

See our website for full descriptions: <http://www.cis.rit.edu/mcsl/SSC>. For more information contact Val Hemink at val@cis.rit.edu or call 585-475-7189.

Published online 23 March 2011 in Wiley Online Library (wileyonlinelibrary.com). DOI 10.1002/col.20707